Drought conditions disrupt atmospheric carbon uptake in a Mediterranean saline lake

Ihab Alfadhel[1,2], Ignacio Peralta-Maraver[1,2,3]*, Isabel Reche[1,2,3], Enrique P. Sánchez-Cañete[2,4,5], Sergio Aranda-Barranco[1,4], Eva Rodríguez-Velasco[1,2,3], Andrew S. Kowalski[2,4,5], Penélope Serrano-Ortiz[1,4]*.

Authors adress:

[1]Departamento de Ecología, Facultad de Ciencias, Universidad de Granada, Granada, Spain.

[2]Instituto del Agua, Granada, Universidad de Granada, Spain.

[3]Research Unit Modeling Nature (MNat), Universidad de Granada, Granada, Spain.

[4]Instituto Interuniversitario de Investigación del Sistema Tierra en Andalucía (IISTA), Universidad de Granada, Spain.

[5]Departamento de Física Aplicada, Universidad de Granada, Granada, Spain.

Correspondence to: Ignacio Peralta-Maraver (*peraltamaraver@ugr.es*) and Penélope Serrano-Ortiz (*penelope@go.ugr.es*).

Abstract: Saline inland lakes play a key role in the global carbon cycle, acting as dynamic zones for atmospheric carbon exchange and storage. Given the global decline of saline lakes and the expected increase of periods of drought in a climate change scenario, changes in their potential capacity to uptake or emit atmospheric carbon are expected. Here, we conducted continuous measurements of CO_2 and CH_4 fluxes at the ecosystem scale in a saline endorheic lake of the Mediterranean region over nearly 2 years. Our focus was on determining net CO_2 and CH_4 exchanges with the atmosphere under both dry and flooded conditions, using the eddy covariance (EC) method. We coupled greenhouse gas flux measurements with water storage and analyzed meteorological variables like air temperature and radiation, known to influence carbon fluxes in lakes. This extensive data integration enabled the projection of the net carbon flux over time, accounting for both dry and wet conditions on an interannual scale. We found that the system acts as a substantial carbon sink by absorbing atmospheric CO_2 under wet conditions. In years with prolonged water storage, it is predicted that the lake's CO_2 assimilation capacity can

33   surpass -0.7 kg C m² annually. Conversely, during extended drought years, a reduction in

34   CO_2 uptake capacity of more than 80% is expected. Regarding CH_4, we measured uptake

35   rates that exceeded those of well-aerated soils such as forest soils or grasslands, reaching

36   values of -0.2 μmol m^{-2} s^{-1}. Additionally, we observed that CH_4 uptake during dry

37   conditions was nearly double that of wet conditions. However, the absence of continuous

38   data prevented us from correlating CH_4 uptake processes with potential environmental

39   predictors. Our study challenges the widespread notion that wetlands are universally

40   greenhouse gas emitters, highlighting the significant role that endorheic saline lakes can

41   play as natural sink of atmospheric carbon. However, our work also underscores the

42   vulnerability of these ecosystem services in the current climate change scenario, where

43   drought episodes are expected to become more frequent and intense in the coming years.

44

45   **Keywords:** Intermittent saline lake, eddy covariance, greenhouse gas fluxes, ecosystem

46   metabolism, Mediterranean shallow lake

47

48   1. Introduction

49   Saline inland lakes are diverse and play a crucial role in the global carbon cycle, serving

50   as dynamic zones for carbon dioxide exchange with the atmosphere (Li et al. 2022; Liao

51   et al. 2024) and long-term sinks of organic and inorganic carbon (Anderson and Stedmon

52   2007; Song et al. 2013; Li et al. 2017). In limnology, however, the ecological importance

53   of these systems has only recently been recognized, despite accounting for approximately

54   44% of global lake volume and 23% of lake surface area (Messager et al., 2016). Saline

55   lakes vary in size from ephemeral ponds to extensive deep-water bodies, such as the

56   Caspian Sea (Eugster and Hardie, 1978). These lakes are characterized by salinity levels

57   that exceed 3 parts per thousand and are notably isolated from a direct marine influence

58   (Williams, 2002; Wang et al., 2018). They are found in endorheic (hydrologically

59   landlocked) basins across a wide array of climates, spanning cold to warm/hot arid

60   regions in all continents, including Antarctica (Williams, 2002; Wang et al., 2018). As

61   terminal points in many hydrological networks, they collect not only significant amounts

62   of salts but also nutrients and organic and inorganic carbon (Anderson and Stedmon 2007;

63   Song et al. 2013; Batanero et al. 2017; Li et al. 2017; Liao et al. 2024).

64   Past estimations about the role of saline lakes on global carbon fluxes suggested

65   that these lakes might function as hotspots for the CO_2 emission (Duarte et al., 2008).

However, more recent works point out that saline lakes have lower partial pressure of CO_2 than freshwater lakes (Wen et al. 2017) and some systems appear to take up CO_2 during the winter (Li et al., 2022) or even annually (Yang et al. 2021) due to physicochemical reactions and increased activity of primary producers. Therefore, more seasonal studies on CO_2 fluxes in saline lakes are needed to understand the conditions when these systems behave as sinks or sources of CO_2. Variations in CO_2 and CH_4 flux estimates across different studies of water bodies are primarily due to the highly variable data obtained from discrete sampling (Li et al. 2022) or because of differences in sampling seasons at the intra-annual scale (Liao et al. 2024). Meanwhile, gathering continuous time series data on CO_2 and CH_4 sequestration and emission fluxes over years is needed for accurate assessment of the net carbon balance in inland water systems (Martínez-García et al. 2024). Nevertheless, long-term, uninterrupted, and direct monitoring of greenhouse gas flux dynamics at the ecosystem level is relatively scarce in aquatic ecosystems, and this is particularly true for saline lakes. To the best of our knowledge, only a couple of studies have reported continuous year-round direct measurements at the ecosystem scale for CO_2 fluxes (Yang et al. 2021; Li et al. 2022). However, saline lakes' characteristics differ with latitude (Hammer 1986) and could have very different behaviors regarding carbon exchanges depending on climate conditions.

The carbon hydrochemistry in permanent saline lakes, especially in mountainous and Arctic latitudes such as the Tibetan Plateau or Svalbard is largely influenced by surface ice formation (Anderson et al., 2004; Rysgaard et al., 2012, 2013; Wu et al., 2014; Yan and Zheng, 2015). In contrast, saline lakes in arid and semi-arid endorheic basins, including Mediterranean climates, are typically shallow, often ephemeral, and/or hypersaline due to evaporation exceeding precipitation (García et al., 1997; Batanero et al. 2017; Saccò et al., 2021). The lower depths and higher surface-to-volume ratio, driven by drought conditions, induce significant physicochemical fluctuations in these saline inland water bodies, spanning from diurnal to interannual scales (Comin et al. 1990; García and Niell 1991; García et al. 1997; Batanero et al. 2017). Consequently, the precipitation regime and subsequent changes in groundwater levels determine the ecology of saline lakes in arid and semi-arid regions. However, research on the interannual variability of carbon fluxes in saline lakes affected by seasonal flooding and drought is lacking. This knowledge gap urgently requires focused research to elucidate the impacts of climatic variability on the carbon dynamics of these ecosystems, which have been identified as particularly vulnerable to climate fluctuations (Tweed et al., 2011).

100 Furthermore, recent studies highlight a global decline in lake water storage in most
101 endorheic basins and in the Sahara, Arabia, and Southern Europe basin in particular
102 (Wang et al. 2018), a situation expected to worsen with more severe droughts in a climate
103 change scenario, leading to lower water levels and prolonged desiccation periods
104 (Wurtsbaugh et al., 2017; Hassani et al., 2020).

105   In this study, we carried out continuous and interannual measurements of CO_2 and
106 CH_4 fluxes at the ecosystem level in Spain's saline lake Fuente de Piedra using the Eddy
107 Covariance (EC) method. Serving as a model of a Mediterranean shallow saline lake, it
108 is characterized by sporadic episodes of water retention but predominantly dry during the
109 summer. It is worth noting that Fuente de Piedra Lake was designated as a Ramsar site in
110 1983, ensuring a rich history of monitoring water storage and the various meteorological
111 drivers of CO_2 and CH_4 fluxes. The objectives of our work are a) to quantify carbon
112 exchanges during the dry and the flooded conditions, determining its role as a carbon
113 source or sink, b) to evaluate main drivers promoting carbon exchange behaviors, and
114 finally c) Using available records of the time series for the main drivers of fluxes to model
115 the annual net carbon flux of the system in the past. Our research aims to enhance our
116 understanding of the carbon dynamics and the impacts of climate change on the net carbon
117 balance in Mediterranean intermittent endorheic lakes.

118

2. Material and methods

120 *Study Site*

121 Fuente de Piedra is a shallow and saline lake located in an endorheic basin in the province
122 of Málaga, Andalusia, Spain (37.11 N, -4.77 W, elevation 410 m: **Fig 1**). It spans
123 approximately 17 km^2, measuring 6.8 km in length and 2.5 km in width, with a maximum
124 depth of 1.5 meters. We take advantage of Fuente de Piedra Lake's inclusion in the
125 Ramsar Convention in 1983. This designation ensures a rich history monitoring of water
126 storage and the meteorological drivers discussed in this article. Such a comprehensive
127 dataset allows for the back projection of the net carbon flux of the system over time,
128 incorporating both dry and wet conditions at an interannual scale. This lake is recognized
129 as a vital habitat within a protected wetland at various levels—regional (as a natural
130 reserve), European (designated as a special bird protection area), and international
131 (acknowledged as a Ramsar site)—and offers an exemplary nesting ground for the pink
132 flamingo (*Phoenicopterus roseus*), largely due to its shallow waters. Among primary

producers, diatoms constitute the largest fraction of primary producers of the phytoplankton all through the year, being dominated by *Hantzschia amphioxys*, *Amphora coffeaiformis*, *Stauronensis amphioxys*, *Cocconeis placentula*, *Entomoneis* sp. and several species of *Navicula* and *Nitzchia* sp. (García and Niell, 1993).

Salinity levels in the lake vary significantly, ranging from oligosaline (5 ppt) to hypersaline conditions (> 200 ppt), influenced by the annual hydrological cycle (Batanero et al. 2017). This cycle is delineated into two distinct phases: a pooling phase during autumn and winter (December to March), and an evaporative and drought phase spanning spring and summer (April to November). The lake primarily receives water from groundwater inflow (Rodríguez- Rodríguez et al. 2006), complemented by contributions from two streams (**Fig. 1**) and surface runoff from surrounding farmlands. Notably, the stream entering from the northeast adds nutrients. However, sediment samples distributed across the lake and analyzed through combustion (Heiri et al., 2001) showed it to be homogeneous in organic carbon (0.21 ±0.07 mg C), nitrogen (0.015±0.004 mg N) and the C:N ratio (14.4± 2.3).

Field measurements of greenhouse gas fluxes and meteorological drivers.

We employed the eddy covariance method to quantify the exchanges of CO_2, CH_4, and energy (sensible and latent heat) every 30 min from August 2021 to May 2023. Thus, the eddy covariance system was operated for more than 21 months, including two dry periods in summer. An open-path eddy covariance (EC) system was strategically positioned atop a tower, 3.1 meters above ground level, on the western bank of the lake (**Fig.1**). This setup included two open-path infrared gas analyzers: the LI7500 for CO_2 and water vapor, and the LI7700 for CH_4 (LICOR Inc., Lincoln, NE, USA). Wind vector components (u, v, w) and sonic temperature were accurately measured using a sonic anemometer (R.M. Young 81000V, Traverse City, MI, USA). These data were recorded on a data logger (CR1000, Campbell Scientific, Logan, UT, USA)at a frequency of 10Hz.

In addition to gas measurements, we measured a comprehensive suite of environmental and soil state variables every 10 seconds to capture the conditions over a representative ground surface area and collected every 30 min average by a data logger (CR1000, Campbell Scientific, Logan, UT, USA). Air temperature (T_a) and relative humidity (RH) were monitored using a thermohygrometer (HMP 45C, Campbell Scientific, Logan, UT, USA). Net radiation (R_n) was quantified by a net radiometer (NR Lite, Kipp and Zonen, Delft, Netherlands). Soil heat flux (G) calculations, including the

167 energy stored in the soil, were facilitated by one heat flux plate (HFP01SC, Hukseflux,
168 Delft, Netherlands) placed at 8 cm depth, complemented by three pairs of soil temperature
169 probes (TCAV, Campbell Scientific, Logan, UT, USA) situated at depths of 4 cm and
170 lateral distances of 3.20 m, 6.34 m, and 8.90 m from the tower.

171   The groundwater level (GWL) was monitored daily using a piezometer situated
172 within a well in the salt flats, approximately 2 kilometres south of the EC tower and on
173 the opposite side of the lake (37.1071° N, -4.7631° W; Fig S1). The location of the
174 piezometer coincides with the central and deepest part of the lake when there is water.
175 Negative GWL values indicate conditions when the lake is entirely lacking surface water.
176 Positive values measured by the piezometer were used to determine the lake depth.
177 Furthermore, data on daily precipitation (PPT), air temperature, and incident solar
178 radiation (spanning wavelengths from 350 to 1100 nm) were acquired from a
179 meteorological station located adjacent to Fuente de Piedra Lake, in Sierra Yeguas
180 (37.1383° N, -4.8358°; 467 m.a.s.l.). The tower setup and instruments were maintained
181 (mainly cleaning lenses of the open path sensors) every two weeks.

182

183 ***Greenhouse gas flux data processing, quality control and partitioning***
184 Half-hourly means (48 measurements per day), variances, and covariances of greenhouse
185 gas fluxes, adhering to the principles of Reynolds decomposition, were calculated using
186 the EddyPro® 7.0.7 software (Li-Cor), according to international standards and protocols
187 (Sabbatini et al., 2018). The data processing protocol encompassed the following steps:
188 (1) axis rotation for tilt correction using the double rotation method (Wilczak et al., 2001),
189 (2) turbulent fluctuations were calculated using block averaging method, (3) time lag was
190 compensated by covariance maximization with default, (4) Webb–Pearman–Leuning
191 (WPL) correction of air density fluctuation (Webb et al., 1980), (5) despiking and raw
192 data statistical screening (Vickers and Mahrt, 1997) and (6) spectral corrections of high-
193 and low-pass filtering effects. Regarding the latter, high-frequency loss due to path
194 averaging, signal attenuation and sensor separation was compensated according to
195 Moncrieff et al., (1997), whereas low-frequency loss due to finite time averaging length
196 and detrending was corrected according to Moncrieff et al. (2004). Quality check flags
197 were calculated for flux data according to the widely adopted methodology combining
198 two tests: steady state test and the developed turbulent conditions test. Over the study
199 period, we only selected high-quality fluxes (flag value =0) measured when the open-path
200 sensors were totally clean according to their respective Automatic Gain Control (AGC)

201   values (AGC value equal to or above 56 for Open path LI-7500A CO_2 /H_2O analyzer and

202   AGC value equal to or higher than 20 for LI-7700).

203   To quantify the sampling area of flux measurements, a footprint model was

204   estimated using the method by Kljun et al., (2004; **Fig 1**). Data periods when the wind

205   came from the terrestrial adjacent environment (251° to 59°) were rejected, representing

206   between 45% and 70% of the available daytime and night-time data respectively during

207   the dry season (GWL=0), and 30% of the available daytime and night-time data

208   respectively during the wet seasons (GWL>0). Overall, for the nearly 2 years of

209   measurements, 18% and 8% of the potential daytime data were of good quality for CO_2

210   and CH_4 fluxes respectively. While for night-time the available data were reduced to 10

211   and 5% respectively. In order to provide additional information regarding the turbulent

212   flux quality (Moncrieff et al 1997), we calculated the energy balance closure (ratio of the

213   sum of sensible and latent turbulent fluxes, H + LE, to the net radiation minus soil heat

214   flux, $R_n − G$) using all the available data during the drought period. The obtained value.

215   was 76% ($R^2 = 0.64$; n = 3117) and is within the range of most the reported FLUXNET

216   sites (Wilson et al 2022; Stoy et al., 2013)

217

218   ***Predicting greenhouse gas fluxes as responses to meteorological drivers***

219   We examine the relationship of CO_2 and CH_4 fluxes in response to groundwater level,

220   serving as a proxy for long-term water storage, with air temperature as the main factor

221   regulating respiration in the system, and incident solar radiation modulating the

222   photosynthetic rate. Since these variables were measured every 24- hours, we processed

223   half-hourly CO_2 and CH_4 fluxes collected to construct 24-hour integrated values. It is

224   important to note that gaps in long-term data records are inevitable when using eddy

225   covariance, primarily due to instrument failure and insufficient turbulence (Falge et al.,

226   2001; Baldocchi et al., 2003; Aubinet et al., 2012). Additionally, data coverage is often

227   reduced when wind originates from undesirable sectors, though this does not necessarily

228   compromise measurement quality (Goloub et al., 2023). Despite these limitations, most

229   studies derive their primary results from annual or seasonal CO_2 and CH_4 balances using

230   various gap-filling procedures. In contrast, we exercise greater caution with our limited

231   data coverage, being very restrictive in quantifying daily fluxes. We selected dates with

232   over 50% of the anticipated data points, particularly those with more than 25 valid

233   measurements well-distributed throughout the day, to calculate integrated daily flux.

234   Before integrating daily flux values, we filled gaps in the half-hourly CO_2 and CH_4 flux

235 data using linear interpolation for missing values. This selection criterion aimed to
236 accurately represent the daily pattern in flux measurement distribution. Then, a
237 trapezoidal integration of the values measured every 30 minutes was performed to
238 calculate the daily flux.

239   To analyze the relationship between integrated daily fluxes and their potential
240 environmental predictors, we employed a linear regression combined with a forward
241 model selection technique (Aho et al 2014). This method involved sequentially fitting a
242 series of regression models, each incorporating different combinations of predictors and
243 their interactions. The process began with simple models, each containing only one
244 primary predictor, and gradually increased in complexity to include all possible
245 interactions among predictors. We then used the Akaike Information Criterion (AIC) to
246 evaluate and identify the most effective model from the set. The model with the lowest
247 AIC was selected as the best fit, indicating it provides the most useful balance between
248 model complexity and explanatory power. After selecting the model, we examined the
249 influence of the predictors by analyzing the slope β coefficients at a significance level of
250 alpha = 0.05, using a 95% confidence interval to determine if these coefficients were
251 significantly different from zero. Additionally, while ground water level (GWL) was
252 measured daily, our model selection process also aimed to identify which daily
253 measurements of air temperature and incident solar radiation (mean, minimum, or
254 maximum) were the best predictors. This method ensured that the chosen model is robust
255 and relevant to the ecological scales being studied.

256   Finally, the chosen candidate model for predicting the fluxes in the system was
257 fitted using available records for the studied drivers, covering the period from 2001 to the
258 present at Fuente de Piedra Lake. This approach aimed to retrospectively model the fluxes
259 in the system. Detailed instructions on how to run these analyses are in the R script
260 available in DRYAD (see details in the *data accessibility statement* section).

261

3. Results

Time series of greenhouse gas emissions and meteorological drivers

264 At Fuente de Piedra Lake, we observed significant seasonal variations in meteorological
265 conditions, as illustrated in **Fig 2A**. Air temperature (T_a) and incident solar radiation
266 exhibited consistent trends throughout the study period, with mean daily values of 17 ± 7
267 °C for T_a and 18 ± 8 MJ m^{-2} d^{-1} for incident solar radiation. In contrast, these two

environmental variables generally followed asynchronous patterns with groundwater level (GWL) and precipitation events, except for a brief peak in precipitation and an increase in GWL between August and September 2021 (Fig. 2A and B). Particularly during the summer months (July, August, September), the highest daily air temperature values coincided with GWLs beneath the surface and a lack of precipitation. Also, during dry conditions, a salt crust several centimeters thick developed on the sediment (see Figure 3B). For instance, the minimum T_a recorded was 2 °C in January 2023 corresponding with a period of frequent precipitation and GWL above the surface. Conversely, the maximum T_a of 34 °C occurred in August 2021, during a period when the GWL was 24 cm below the surface.

After the study period, we were able to collect 4,128 measurements for CO_2 fluxes and 2,425 measurements for CH_4 fluxes, which were relatively well-distributed over the study period. We observed a strong correspondence between water storage in Fuente de Piedra Lake and its capacity to assimilate atmospheric CO_2. The CO_2 flux patterns can be categorized into two distinct lake states: a flooded lake (groundwater level >0 cm, indicated from purple to blue colour in **Fig 2C and D**) and a dry lake (groundwater level <0 cm, shown from orange to yellow colour). During flooding conditions, the lake acted as a CO_2 sink, with fluxes ranging from 0 to -30 μmol m^{-2} s^{-1}. The CO_2 assimilation capacity increases with groundwater level and incident solar radiation, particularly from January to June. Notably, the flooded conditions in the two years of the study showed marked differences in groundwater level. In 2022, we recorded the highest CO_2 uptake of 30 μmol m^{-2} s^{-1} and an averaged value of -3.11 μmol m^{-2} s^{-1} during May, when the groundwater level was at its peak, 40 cm above the surface. This period was also characterized by high variability in CO_2 flux, occasionally showing peaks of CO_2 outgassing approaching 20 μmol m^{-2} s^{-1}. The peak CO_2 uptake in 2023 was approximately half of what was observed in 2022. Although this peak occurred in March rather than May, it followed a similar trend to the ground water level (GWL), which was also about half of the peak level observed in 2022 (~20 cm above the surface) resulting in averaged CO_2 uptake values of -3.66 μmol m^{-2} s^{-1}. In contrast, under dry conditions, Fuente de Piedra Lake ceases CO_2 uptake, occasionally transitioning to minor CO_2 emissions. Notice that during extreme rainfall pulses within dry conditions, when Fuente de Piedra Lake remained relatively dry with the groundwater level below the surface, we observed notable net CO_2 emissions. For example, a heavy rainfall event in September 2021 (36 mm day^{-1}) resulted in CO_2 emissions reaching up to 10 μmol m^{-2} s^{-1}, with a high elevation

302   of the groundwater level above the surface (from -20 to near 20 cm). Also, in October of

303   both 2021 and 2022, subsequent rainfall events (12 mm day^{-1} and 22 mm day^{-1},

304   respectively) corresponded with CO_2 emissions of 7 µmol m^{-2} s^{-1} and 5.5 µmol m^{-2} s^{-1},

305   respectively. In these cases, emissions occurred under negative GWL conditions.

306   In the case of CH_4, the flux was relatively stable throughout the whole study

307   period, generally acting as a sink, with values fluctuating between -0.2 and 0.1 µmol m^{-2}

308   s^{-1} and an average of -0.05 µmol m^{-2} s^{-1} for the study period (**Fig 2D**). Furthermore, the

309   measured CH_4 fluxes did not seem to align clearly with the meteorological variables

310   examined (**Fig S1**).

311

Fluxes of CO_2 and CH_4 at a daily scale

313   When examining the daily scale during wet conditions, it becomes evident that CO_2

314   assimilation predominantly takes place during daylight hours, specifically between 9 a.m.

315   and 2 p.m. (local time) (**Fig. 3**). It should be noted that the few emission values observed

316   within this time frame correspond to the emission occurrences described earlier for the

317   dry season, which promptly followed rainfall events. In the case of dry condition, it is

318   noteworthy that a salt crust forms over the lake, leading to a near cessation of CO_2 fluxes.

319   In the case of CH_4, there is also a discernible increase in assimilation fluxes between 9

320   a.m. and 2 p.m. This observed pattern is consistent in both wet and dry conditions.

321

Model predictions of 24-hour integrated flux values in the study system

323   No evident relationship between CH_4 flux and the environmental predictors studied was

324   found during the study period. Additionally, measurements obtained from the EC tower

325   resulted in a substantial number of gaps in the CH_4 time series, making it impossible to

326   establish a predictive model for these fluxes. On the contrary, we were able to adjust a

327   robust regression model for CO_2 integrated daily flux. A total of 26 daily integrated CO_2

328   flux values were obtained for the sampling period, analyzing those dates when more than

329   25 valid measurements were available. After AIC model selection routine, the candidate

330   predictive model for daily integrated CO_2 flux was determined to include groundwater

331   level, maximum daily air temperature, and mean incident solar radiation. Additionally,

332   the model incorporated interactions between groundwater level and maximum daily air

333   temperature, as well as between groundwater level and incident solar radiation (Summary

334   Table of the model is available in the Supplementary Material). Indeed, fitted statistical

335   model has a relatively high explanatory capability (Adjusted R^2 =0.73).

The model confirmed a positive effect of groundwater level on enhancing CO_2 assimilation in the system (**Fig 4A**; β_{GWL} = -0.115, 95% CI = -0.214 to -0.016; note that assimilation corresponds with negative values of the CO_2 flux). While the isolated impact of air temperature increase on CO_2 assimilation could not be determined (β_{Ta} = +0.07, 95%CI = -0.053 to +0.192), the model identified an antagonistic interaction between air temperature and groundwater level ($\beta_{GWL \times Ta}$ = +0.010, 95%CI = +0.005 to +0.015). As air temperature increases, the positive effect of GWL on CO_2 asimilation diminishes (**Fig 4B**). Conversely, mean daily incident solar radiation was found to promote CO_2 assimilation (β_{Rad} = -0.12, 95%CI = -0.21 to -0.03), with a pronounced synergy between mean daily incident solar radiation and the presence of water ($\beta_{GWL \times Rad}$ = 95%CI = -0.0116 to -0.003), notably enhancing the capacity for CO_2 assimilation (**Fig 4C**).

Using time series data for groundwater level, daily maximum air temperature, and mean daily incident solar radiation at Fuente de Piedra Lake, we generated retrospective predictions of CO_2 assimilation capacity in the system dating back to 2001 (**Fig 4D**). The model predictions closely aligned with the observed values for the study period when using the time series data for the predictors, supporting the robust predictive ability of our model (Supplementary Material; **Fig S2**). Our estimates indicate a pronounced fluctuation in CO_2 assimilation capacity according to hydrological variations. In years with higher groundwater level and prolonged water storage the model predicted an exceptionally high capacity for atmospheric CO_2 assimilation of the lake, with annual values surpassing 0.7 Kg C m^{-2} year^{-1} (e.g., in 2011, 2012, 2014, 2020). In contrast, during years marked by extended droughts, a substantial reduction in CO_2 assimilation capacity was modeled, with predicted reductions exceeding 80% compared to wetter years (Fig. 4D). These drought periods, resulted in a reduction of the assimilation capacity to less than a third of the levels recorded in wet years (e.g., from 2006 to 2010).

4. Discussion

In agreement with previous research on permanent saline lakes of the Tibetan plateau (Li et al. 2022), we demonstrate that a model Mediterranean shallow saline lake serves as a substantial carbon sink, absorbing atmospheric CO_2 when flooded. In particularly wet years, expected uptake values can exceed -1.2 kg C m^{-2} year^{-1}. Sporadic instances were also observed where the system acted as a CO_2 emitter, resulting from rewetting events that followed rainfall during dry conditions. Conversely, CO_2 uptake ceases during dry

369   conditions, reducing the system's capacity in dry years to below -0.2 kg C m^{-2} $year^{-1}$.

370   Longitudinal time series analysis reveals that prolonged droughts indeed hinder the ability

371   of the system to assimilate atmospheric CO_2 due to the lack of water, but we also observed

372   that an increase in air temperature during wet conditions moderates the CO_2 net

373   assimilation capacity, a process likely related to the reduction of gas water solubility with

374   temperature. This underscores the pronounced impact of seasonal and interannual

375   variability, ultimately dictated by drought and rainfall patterns, on the ability of the

376   studied system to sequester atmospheric carbon. Moreover, this pattern also displayed

377   considerable variability at the daily scale, closely correlating with fluctuations in incident

378   solar radiation over daily cycles. In this regard, the CO_2 assimilation capacity of the

379   system peaked during those hours of maximum incident solar radiation. While

380   measurement of CO_2 (and CH_4) fluxes at multiple scales is challenging and requires

381   specialized equipment (i.e. eddy covariance sensors), our research proposes an alternative

382   proxy. By integrating data from environmental predictors at various scales we have been

383   able to reconstruct the behavior of CO_2 exchanges between Fuente de Piedra Lake and

384   the atmosphere. In essence, we estimate CO_2 flux through the continuous measuring of

385   accessible environmental variables, namely, the amount of water, air temperature, and

386   incident solar radiation.

387   In shallow, well-mixed, and oxygenated systems like Fuente de Piedra Lake, the

388   photosynthetic capacity of the phytoplankton community is closely linked to the water

389   column height (i.e. groundwater level; Batanero et al. 2017), promoting CO_2 assimilation

390   as the extent of the habitat for these communities expands (Wetzel, 2001). Related to the

391   aforementioned, a significant synergy exists between water storage in the ecosystem and

392   incident radiation, serving as a proxy for the photosynthetically active radiation upon

393   which photosynthesis depends. This interaction occurs on both a daily scale, associated

394   with variations in light intensity following day-night cycles, and an annual seasonal scale,

395   largely determined by changes in daylight hours throughout the year. Notably, during the

396   night, the net exchange of CO_2 between the water and the atmosphere in Fuente de Piedra

397   Lake is negligible. This could be attributed to the absence of photosynthesis during

398   nighttime. Additionally, the high salinity inherent to these environments constrains

399   methanogenesis, which is the least energy-efficient carbon mineralization process in the

400   redox sequence (reviewed in Soued et al., 2024). Considering the above, it appears to

401   offer a plausible explanation for why microbial respiration does not surpass inorganic

402   carbon assimilation through photosynthesis in systems like Fuente de Piedra Lake during

403   wet conditions, despite the high content of dissolved organic carbon ranging between

404   1.00 and 13.59 mmol C L^{-1} (Batanero et al., 2017).

405   What is more, despite the limited CH_4 flux data, our results position Fuente de

406   Piedra Lake as a CH_4 sink. Rough estimates determined that Fuente de Piedra could take

407   up on average 1.83 mg C m^{-2} day^{-1} and 3.70 mg C m^{-2} day^{-1} during wet and the dry

408   conditions respectively (Supplementary Material; **Fig S3**). Such values are even higher

409   than those measured in typical well aerated soils as in forests or grasslands, with average

410   rates of 0.4-1.26 mg C m^{-2} day^{-1} (Murguia-Flores et al., 2021; Perez-Quezada et al., 2021).

411   Twice the value of uptake during dry conditions compared to wet ones appear to be

412   consistent with some proposed mechanisms promoting CH_4 reduction according to the

413   existing literature, since the increase of temperature together with gas diffusivity due to

414   loss of water, may increase methane oxydation in a similar way to terrestrial ecosystems

415   (Chen et al., 2010; Rafalska et al 2023). However, caution is needed when interpreting

416   our results, as the dynamics of methane fluxes could become very complex in an

417   intermittent system like Fuente de Piedra. On the one hand, just as methanogenic activity

418   is inhibited by salinity (Herbert et al., 2015), methanotrophic activity has also been

419   observed to be significantly reduced by salinity in terrestrial systems (Ho et al., 2018).

420   However, methane oxydation processes associated with aquatic prokaryotes may be more

421   resistant to salinity (Khmelenina et al., 2010; Deng et al. 2017), especially if the variation

422   is gradual (Osudar et al., 2017). Thus, further measurements and analysis are needed to

423   estimate the role of methane oxydation and the relevance of saline intermitent lakes as

424   CH_4 sinks in a climate change scenario.

425   Drought conditions are accompanied by an increase in air temperature, with the

426   high air temperatures recorded immediately before the system completely dries out. We

427   have found that this rise in air temperature leads to a reduction of the system's capacity

428   to assimilate CO_2, even during wet conditions. A direct consequence of climatic warming

429   is the reduction of gas solubility accentuated in saline wetlands (Batanero et al. 2022). In

430   addition, an increase in temperature can enhance microbial metabolic rates and therefore,

431   biomass-specific CO_2 production (Smith et al. 2019). Given that endorheic saline lakes

432   are fueled by significant amounts of organic matter (Li et al., 2017; Batanero et al., 2017;

433   Song et al., 2013), it is unsurprising that warming leads to a decrease in net primary

434   production in the system as a result of enhanced microbial respiration, and consequently,

435   a reduction in CO_2 assimilation capacity. In addition, carbon emissions in inland waters

436   could increase with warming, independently of organic carbon inputs, simply because the

apparent activation energy is predicted to be higher for respiration than photosynthesis (Yvon-Durocher et al. 2010; Yvon-Durocher et al. 2012). Finally, it has been recognized that photosynthesis is often the first process to be affected by environmental stressors, with photosynthetic capacity diminishing prior to other cellular functions (Feller, 2016; Cardona et al., 2018). Specifically, carbon assimilation through the Calvin–Benson cycle exhibits particular vulnerability to both drought and elevated temperatures, occurring even when photosynthetic electron transport continues to operate effectively (Sharkey, 2005). On the whole, we show the profound synergy between global warming and intensifying drought severity and frequency, disrupting the CO_2 assimilation capacity of Mediterranean saline lakes and leading to negative feedback loops.

While the desiccation of saline lakes is not novel, with researchers highlighting the concerning increase in dry periods within many of these ecosystems over recent decades (Williams 1993; Gross 2017; Wurtsbaugh et al. 2017; Wang et al. 2018), our study underscores the significant implications this trend has for the ecosystem services they support. Our retrospective predictions show that in wet years, the system could exhibit a high CO_2 assimilation rate. For instance, between 2010 and 2015, we estimated that Fuente de Piedra Lake had an average assimilation rate of 0.83 (SD = ±0.27) kg C m^{-2} year^{-1}, within the same range as the net assimilation observed in evergreen or deciduous forest systems worldwide (Pastorello et al., 2020) and marine salt marshes (Mayen et al. 2024). Considering the 13.6 km² area of Fuente de Piedra and assuming a constant flux across the lake surface when flooded, we could estimate around 11 tons of carbon sequestered during a wet and fully flooded year. Although this upscaling exercise is crude, it highlights that Mediterranean shallow saline lakes could be a substantial carbon sink and underline the potential relevance of keep them with water during their conservation policies. Therefore, further studies across different Mediterranean shallow saline lakes are necessary to refine these estimates and enhance our understanding of their role in the global scale carbon budget.

5. Conclusion

Our result challenges the generalised belief that inland waters primarily act as sources of greenhouse gases (Raymond et al. 2013). Conversely, the system undergoes significant reductions in its annual atmospheric CO_2 sequestration capacity during dry conditions. For instance, under severe drought conditions as observed in Fuente de Piedra from 2005

470 to 2009, the annual CO_2 sequestration is estimated to have fallen to less than a quarter of
471 what was observed in more humid conditions. Climate change projections, including even
472 the most optimistic scenarios, forecast an increase in both the frequency and duration of
473 heatwaves and droughts in the coming years (Trenberth 2011, Perkins-Kirkpatrick 2020).
474 This implies that saline lake ecosystems in arid and semi-arid endorheic basins will
475 remain dry for longer periods, or may even vanish, resulting in the loss of a significant
476 carbon sequestration pathway. Importantly, the disappearance of saline lakes due to water
477 scarcity has been largely attributed to anthropogenic water overuse (i.e., agriculture)
478 rather than to macroclimatic phenomena (Wurtsbaugh et al. 2017). This seems to be the
479 case of Fuente de Piedra Lake, as the catchment area is dominated by agricultural land.
480 Thus, a proper water system management during drought conditions seems to be the most
481 plausible solution to preserve the ecosystem services provided by Mediterranean saline
482 lakes.
483

Author contribution

485 PS-O and IR conceived the study; all authors contributed to the installation and
486 maintenance of the eddy covariance tower; IA led the fieldwork and the processing of the
487 samples with the help of the rest of the authors; IP-M carried out the analyses and the
488 preparation of the results; IA, IP-M, and PS-O conducted the preparation of the first draft
489 of the work; all authors participated in the drafting of the final draft.
490

Data accessibility statement

492 The R script used to conduct the data analysis and the datasets are available at the Dryad
493 Digital Repository:
494 https://datadryad.org/stash/share/qEpPRJopVR132UszL3bnaxoZh07ADL0E5LpVL6xC
495 SZA
496

Acknowledgements

498 We thank the logistic support and groundwater level data provided by the curator of the
499 Natural Reserve of Laguna de Fuente de Piedra África Lupión Sánchez. Author also
500 acknowledge the review provided by the anonymous reviewers.
501

Financial support

503   This work was partially support by the projects PID2020-117825GB-C21 and PID2020-

504   117825GB-C22 funded by MCIN/AEI/10.13039/501100011033, LifeWatch-2019-10-

505   UGR-01 and LifeWatch-2019-09-CSIC-13 funded by the MCIN through the FEDER

506   funds from the Spanish Pluriregional Operational Program 2014-2020 (POPE),

507   LifeWatch-ERIC action line and project BAGAMET (P20_00016) funded by the

508   Counseling of Economy, Innovation, Science and Employment from the Government of

509   Andalucía, including European Union ERDF funds. I.P.-M. developed his research as

510   part of the eWARM project, supported by the Marie Skłodowska-Curie postdoctoral

511   fellowship 2022 (project number 101110111).

512

Competing interests

514   The authors declare that they have no conflict of interest.

515

References

517   Aho, K., Derryberry, D., and Peterson, T: Model selection for ecologists: the worldviews

518   of AIC and BIC. Ecology, 95(3), 631-636, https://doi.org/10.1890/13-1452.1 ,

519   2014.

520   Anderson, L. G., Falck, E., Jones, E. P., Jutterström, S., and Swift, J. H: Enhanced uptake

521   of atmospheric CO_2 during freezing of seawater: A field study in Storfjorden,

522   Svalbard.   J.   Geophys.   Res.   Oceans,   109(C6)

523   https://doi.org/10.1029/2003JC002120, 2024.

524   Anderson, N. J., and Stedmon, C. A: The effect of evapoconcentration on dissolved

525   organic carbon concentration and quality in lakes of SW Greenland. Freshwater

526   Biology, 52(2), 280-289, https://doi.org/10.1111/j.1365-2427.2006.01688.x ,

527   2007.

528   Aubinet, M., Vesala, T., and Papale, D. Eddy covariance: A practical guide to

529   measurement and data analysis. London, UK Springer, 2012.

530   Baldocchi, D. D. Assessing the eddy covariance technique for evaluating carbon dioxide

531   exchange rates of ecosystems: past, present and future. Glob. Chan. Biol. 9(4),

532   479-492, https://doi.org/10.1046/j.1365-2486.2003.00629.x , 2003.

533   Batanero, G. L., León-Palmero, E., Li, L., Green, A. J., Rendón-Martos, M., Suttle, C.

534   A., and Reche, I. Flamingos and drought as drivers of nutrients and microbial

dynamics in a saline lake. Scientific Reports, 7(1), 12173, https://doi.org/10.1038/s41598-017-12462-9 , 2017.

Batanero, G. L., Green, A. J., Amat, J. A., Vittecoq, M., Suttle, C. A., and Reche, I. Patterns of microbial abundance and heterotrophic activity along nitrogen and salinity gradients in coastal wetlands. Aquatic Sciences, 84, 22, https://doi.org/10.1007/s00027-022-00855-6, 2022.

Cardona, T., Shao, S., and Nixon, P. J: Enhancing photosynthesis in plants: the light reactions. Essays in biochemistry, 62(1), 85-94, https://doi.org/10.1042/EBC20170015 , 2018.

Chen, W., Wolf, B., Zheng, X., Yao, Z., Butterbach-bahl, K. L. A. U. S., Brueggemann, N., ... and Han, X: Annual methane uptake by temperate semiarid steppes as regulated by stocking rates, aboveground plant biomass and topsoil air permeability. Glob. Change Biol., 17(9), 2803-2816. https://doi.org/10.1111/j.1365-2486.2011.02444.x , 2011.

Comín, F. A., Julia, R., Comin, M. P., and Plana, F: Hydrogeochemistry of Lake Gallocanta (Aragón, NE Spain). In Saline Lakes: Proceedings of the Fourth International Symposium on Athalassic (inland) Saline Lakes, held at Banyoles, Spain, May 1988 (pp 51-66). Springer Netherlands, 1990

Deng, Y., Liu, Y., Dumont, M., and Conrad, R. Salinity affects the composition of the aerobic methanotroph community in alkaline lake sediments from the Tibetan Plateau. Microb. Ecol., 73, 101-110, https://doi.org/10.1007/s00248-016-0879-5 , 2017.

Duarte, C. M., Prairie, Y. T., Montes, C., Cole, J. J., Striegl, R., Melack, J., and Downing, J. A: CO2 emissions from saline lakes: A global estimate of a surprisingly large flux. J. Geophys. Res. G: Biogeosciences, 113(G4), https://doi.org/10.1029/2007JG000637 , 2008.

Eugster, H. P., and Hardie, L. A. (1978). Saline lakes. In Lakes: chemistry, geology, physics (pp. 237-293). New York, NY: Springer New York.

Falge, E., Baldocchi, D., Olson, R., Anthoni, P., Aubinet, M., Bernhofer, C., ... & Wofsy, S. Gap filling strategies for long term energy flux data sets. Agric. For. Meteorol. 107(1), 71-77, https://doi.org/10.1016/S0168-1923(00)00235-5 , 2001.

Feller, U: Drought stress and carbon assimilation in a warming climate: Reversible and irreversible impacts. J. Plant Physiol., 203, 84-94, https://doi.org/10.1016/j.jplph.2016.04.002 , 2016.

569 García, C. M., García-Ruiz, R., Rendón, M., Niell, F. X., and Lucena, J: Hydrological
570   cycle and interannual variability of the aquatic community in a temporary saline
571   lake (Fuente de Piedra, Southern Spain). Hydrobiologia, 345, 131-141,
572   https://doi.org/10.1023/A:1002983723725 , 1997.

573 Garcia, C. M., and Niell, F. X: Burrowing beetles of the genus Bledius (Staphylinidae) as
574   agents of bioturbation in the emergent areas and shores of an athalassic inland lake
575   (Fuente de Piedra, southern of Spain). Hydrobiologia, 215, 163-173,
576   https://doi.org/10.1007/BF00014719 , 1991.

577 García, C. M., and Niell, F. X: Seasonal change in a saline temporary lake (Fuente de
578   Piedra, southern Spain). Hydrobiologia, 267(1), 211-223,
579   https://doi.org/10.1007/BF00018803 ,1993.

580 Golub, M., Koupaei-Abyazani, N., Vesala, T., Mammarella, I., Ojala, A., Bohrer, G., et
581   al. Diel, seasonal, and inter-annual variation in carbon dioxide effluxes from lakes
582   and reservoirs. Environ. Res. Lett. 18(3), 034046, https://doi.org/10.1088/1748-
583   9326/acb834 , 2023.

584 Guerrero, M. C., and Wit, R. d: Microbial mats in the inland saline lakes of Spain.
585   Limnetica, 8, 197–204, 1992.

586 Hammer, U. T: Saline lake ecosystems of the world. Springer Science and Business
587   Media, 1986.

588 Hardie, L. A., Smoot, J. P., and Eugster, H. P: Saline lakes and their deposits: a
589   sedimentological approach. Modern and ancient lake sediments, 7-41, 1978.

590 Hassani, A., Azapagic, A., D'Odorico, P., Keshmiri, A., and Shokri, N: Desiccation crisis
591   of saline lakes: A new decision-support framework for building resilience to
592   climate change. Sci. Total Environ., 703, 134718,
593   https://doi.org/10.1016/j.scitotenv.2019.134718 , 2020.

594 Heiri, O., Lotter, A. F., and Lemcke, G.: Loss on ignition as a method for estimating
595   organic and carbonate content in sediments: reproducibility and comparability of
596   results. J. Paleolimnol., 25, 101-110, https://doi.org/10.1023/A:1008119611481 ,
597   2001.

598 Khmelenina, V. N., Shchukin, V. N., Reshetnikov, A. S., Mustakhimov, I. I., Suzina, N.
599   E., Eshinimaev, B. T., and Trotsenko, Y. A.: Structural and functional features of
600   methanotrophs from hypersaline and alkaline lakes. Microbiology, 79, 472-482,
601   https://doi.org/10.1134/S0026261710040090, 2010.

Kljun, N., Calanca, P., Rotach, M. W., and Schmid, H. P.: A simple parameterisation for flux footprint predictions. Bound-Lay Meteorol., 112(3), 503–523, https://doi.org/10.1023/B:BOUN.0000030653.71031.96 , 2004.

Ho, A., Mo, Y., Lee, H. J., Sauheitl, L., Jia, Z., and Horn, M. A. Effect of salt stress on aerobic methane oxidation and associated methanotrophs; a microcosm study of a natural community from a non-saline environment. Soil Biol. Biochem., 125, 210-214, https://doi.org/10.1016/j.soilbio.2018.07.013 , 2018.

Li, Y., Zhang, C., Wang, N., Han, Q., Zhang, X., Liu, Y., Xu, L. and Ye, W: Substantial inorganic carbon sink in closed drainage basins globally. Nature Geosci., 10(7), 501-506, https://doi.org/10.1038/ngeo2972 ,2017.

Li, X. Y., Shi, F. Z., Ma, Y. J., Zhao, S. J., and Wei, J. Q: Significant winter CO_2 uptake by saline lakes on the Qinghai-Tibet Plateau. Glob. Change Biol., 28(6), 2041–2052, https://doi.org/10.1111/gcb.16054 , 2022.

Liao, Y., Xiao, Q., Li, Y., Yang, C., Li, J., and Duan, H: Salinity is an important factor in carbon emissions from an inland lake in arid region. Sci. Total Environ., 906, 167721, https://doi.org/10.1016/j.scitotenv.2023.167721 , 2024.

Martínez-García, A., Peralta-Maraver, I., Rodríguez-Velasco, E., Batanero, G.L., García-Alguacil, M., Picazo, F., Calvo, J., Morales-Baquero, R., Rueda, F.J., Reche, R: Particulate organic carbon sedimentation triggers lagged methane emissions in a eutrophic reservoir. Limnol. Oceanogr. Lett., https://doi.org/10.1002/lol2.10379 , 2024.

Messager, M. L., Lehner, B., Grill, G., Nedeva, I., and Schmitt, O: Estimating the volume and age of water stored in global lakes using a geo-statistical approach. Nature comm., 7(1), 13603, https://doi.org/10.1038/ncomms13603, 2016.

Moncrieff, J. B., Massheder, J. M., de Bruin, H., Elbers, J., Friborg, T., Heusinkveld, B., Kabat, P., Scott, S., Soegaard, H., and Verhoef, A.: A system to measure surface fluxes of momentum, sensible heat, water vapour and carbon dioxide. J. Hydrol., 188–189, 589–611, https://doi.org/10.1016/S0022-1694(96)03194-0 ,1997.

Moncrieff, J., Clement, R., Finnigan, J., and Meyers, T: Averaging, Detrending, and Filtering of Eddy Covariance Time Series. In Handbook of Micrometeorology (pp. 7–31), 2004.

Murguia-Flores, F., Ganesan, A. L., Arndt, S., and Hornibrook, E. R.: Global uptake of atmospheric methane by soil from 1900 to 2100. Global Biogeochem. Cycles, 35(7), e2020GB006774, https://doi.org/10.1029/2020GB006774 , 2021.

636 Osudar, R., Klings, K. W., Wagner, D., and Bussmann, I.: Effect of salinity on microbial

637   methane oxidation in freshwater and marine environments. Aquatic Microb. Ecol.,

638   80(2), 181-192, https://doi.org/10.3354/ame01845 , 2017.

639 Pastorello, G., Trotta, C., Canfora, E., Chu, H., Christianson, D., Cheah, Y. W., ... & Law,

640   B.: The FLUXNET2015 dataset and the ONEFlux processing pipeline for eddy

641   covariance data. Sci. Data, 7, 225, https://doi.org/10.1038/s41597-020-0534-3,

642   2020.

643 Perez-Quezada, J. F., Urrutia, P., Olivares-Rojas, J., Meijide, A., Sánchez-Cañete, E. P.,

644   and Gaxiola, A.: Long term effects of fire on the soil greenhouse gas balance of

645   an old-growth temperate rainforest. *Sci. Total Environ.*, 755, 142442,

646   https://doi.org/10.1016/j.scitotenv.2020.142442 , 2021.

647 Perkins-Kirkpatrick, S. E., and Lewis, S. C.: Increasing trends in regional heatwaves.

648   Nature comm., 11(1), 3357, https://doi.org/10.1038/s41467-020-16970-7 , 2020.

649 Rafalska, A., Walkiewicz, A., Osborne, B., Klumpp, K., and Bieganowski, A.: Variation

650   in methane uptake by grassland soils in the context of climate change–A review

651   of effects and mechanisms. Sci. Total Environ., 871, 162127,

652   https://doi.org/10.1016/j.scitotenv.2023.162127 , 2023.

653 Raymond, P. A., Hartmann, J., Lauerwald, R., Sobek, S., McDonald, C., Hoover, M., ...

654   and Guth, P.: Global carbon dioxide emissions from inland waters. Nature,

655   503(7476), 355-359, https://doi.org/10.1038/nature12760 , 2013.

656 Rodríguez- Rodríguez, M., Benavente, J. and Moral, F.: High density ground-water flow,

657   major-ion chemistry and field experiments in a closed basin: Fuente de Piedra

658   Playa Lake (Spain). American J. Environ. Sciences. 1, 164–171, 2006.

659 Rysgaard, S., Glud, R. N., Lennert, K., Cooper, M., Halden, N., Leakey, R. J. G., and

660   Barber, D.: Ikaite crystals in melting sea ice–implications for pCO2 and pH levels

661   in Arctic surface waters. The Cryosphere, 6(4), 901–908,

662   https://doi.org/10.5194/tc-6-901-2012 , 2012.

663 Rysgaard, S., Søgaard, D. H., Cooper, M., Pućko, M., Lennert, K., Papakyriakou, T. N.,

664   and Barber, D.: Ikaite crystal distribution in Arctic winter sea ice and implications

665   for CO2 system dynamics. The Cryosphere, 7(2), 707–718,

666   https://doi.org/10.5194/tc-7-707-2013 , 2013.

667 Saccò, M., White, N. E., Harrod, C., Salazar, G., Aguilar, P., Cubillos, C. F., ... and

668   Allentoft, M. E. Salt to conserve: A review on the ecology and preservation of

669   hypersaline   ecosystems.   Biol.   Rev.,   96(6),   2828-2850,
670   https://doi.org/10.1111/brv.12780 , 2021.

671 Sabbatini, S., Mammarella, I., Arriga, N., Fratini, G., Graf, A., Hörtnagl, L., Ibrom, A.,
672   Longdoz, B., Mauder, M., Merbold, L., Metzger, S., Montagnani, L., Pitacco, A.,
673   Rebmann, C., Sedlák, P., Šigut, L., Vitale, D., and Papale, D.: Eddy covariance
674   raw data processing for CO2 and energy fluxes calculation at ICOS ecosystem
675   stations. Int. Agrophysics., 32(4), 495–515, https://doi.org/10.1515/intag-2017-
676   0043 , 2018.

677 Sharkey, T. D.: Effects of moderate heat stress on photosynthesis: importance of
678   thylakoid reactions, rubisco deactivation, reactive oxygen species, and
679   thermotolerance provided by isoprene. Plant Cell Environ. 28(3), 269-277,
680   https://doi.org/10.1111/j.1365-3040.2005.01324.x , 2005.

681 Smith, T. P., Thomas, T. J., García-Carreras, B., Sal, S., Yvon-Durocher, G., Bell, T., and
682   Pawar, S.: Community-level respiration of prokaryotic microbes may rise with
683   global warming. Nature comm., 10(1), 5124, https://doi.org/10.1038/s41467-019-
684   13109-1 , 2019.

685 Song, K. S., Zang, S. Y., Zhao, Y., Li, L., Du, J., Zhang, N. N., ... and Liu, L.:
686   Spatiotemporal characterization of dissolved carbon for inland waters in semi-
687   humid/semi-arid region, China. Hydrol. Earth Syst. Sci., 17(10), 4269-4281,
688   https://doi.org/10.5194/hess-17-4269-2013 , 2013.

689 Soued, C., Bogard, M. J., Finlay, K., Bortolotti, L. E., Leavitt, P. R., Badiou, P., ... and
690   Kowal, P.: Salinity causes widespread restriction of methane emissions from small
691   inland waters. Nature Comm., 15(1), 717, https://doi.org/10.1038/s41467-024-
692   44715-3 , 2024.

693 Stoy, P. C., Mauder, M., Foken, T., Marcolla, B., Boegh, E., Ibrom, A., Arain, M. A.,
694   Arneth, A., Aurela, M., Bernhofer, C., Cescatti, A., Dellwik, E., Duce, P.,
695   Gianelle, D., van Gorsel, E., Kiely, G., Knohl, A., Margolis, H., Mccaughey, H.,
696   … Varlagin, A.: A data-driven analysis of energy balance closure across
697   FLUXNET research sites: The role of landscape scale heterogeneity. Agric. For.
698   Meteorol., 171–172, 137–152, https://doi.org/10.1016/j.agrformet.2012.11.004 ,
699   2013

700 Trenberth, K. E.: Changes in precipitation with climate change. Clim. Res. 47(1-2), 123-
701   138, https://doi.org/10.3354/cr00953 , 2011.

702 Tweed, S., Grace, M., Leblanc, M., Cartwright, I., and Smithyman, D.: The individual
703   response of saline lakes to a severe drought. Sci. Total Environ., 409(19), 3919-
704   3933, https://doi.org/10.1016/j.scitotenv.2011.06.023 ,2011.

705 Vickers, D., and Mahrt, L.: Quality control and flux sampling problems for tower and
706   aircraft   data.   J.   Atmos.   Ocean.   Techno.,   14(3),   512–526.,
707   https://doi.org/10.1175/1520-0426(1997)014<0512:QCAFSP>2.0.CO;2 , 1997.

708 Wang, J., Song, C., Reager, J. T., Yao, F., Famiglietti, J. S., Sheng, Y., ..., and Wada, Y.:
709   Recent global decline in endorheic basin water storages. Nature Geosci 11, 926–
710   932, https://doi.org/10.1038/s41561-018-0265-7 , 2018.

711 Webb, E. K., Pearman, G. I., and Leuning, R. Correction of flux measurements for density
712   effects due to heat and water vapour transfer. Q. J. R. Meteorol. Soc. 106 (447),
713   85–100, https://doi.org/10.1002/qj.49710644707 ,1980

714 Wen, Z., Song, K., Shang, Y., Fang, C., Li, L., Lv, L., ... and Chen, L.: Carbon dioxide
715   emissions from lakes and reservoirs of China: a regional estimate based on the
716   calculated pCO_2.   Atmos.   Environ.,   170,   71-81,
717   https://doi.org/10.1016/j.atmosenv.2017.09.032 , 2017.

718 Williams, W. D.: Environmental threats to salt lakes and the likely status of inland saline
719   ecosystems   in   2025.   Environ.   Conserv.,   29(2),   154-167,
720   https://doi.org/10.1017/S0376892902000103 , 2002.

721 Wilson, K., Goldstein, A., Falge, E., Aubinet, M., Baldocchi, D., Berbigier, P., ... &
722   Verma, S.: Energy balance closure at FLUXNET sites. Agricultural and Forest
723   Meteorology, 113(1–4), 223–243, https://doi.org/10.1016/S0168-1923(02)00109-
724   0 , 2002.

725 Wu, Y., Wang, N., Zhao, L., Zhang, Z., Chen, L. I., Lu, Y., Lü, X., and Chang, J.:
726   Hydrochemical characteristics and recharge sources of Lake Nuoertu in the
727   Badain Jaran Desert. Sci. Bull., 59(9), 886–895 , https://doi.org/10.1007/s11434-
728   013-0102-8 , 2014.

729 Wurtsbaugh, W. A., Miller, C., Null, S. E., DeRose, R. J., Wilcock, P., Hahnenberger,
730   M., ... and Moore, J.: Decline of the world's saline lakes. Nat. Geosci., 10(11),
731   816-821, https://doi.org/10.1038/ngeo3052 , 2017

732 Yan, L., and Zheng, M.: Influence of climate change on saline lakes of the Tibet Plateau,
733   1973–2010.   Geomorphology,   246,   68-78,
734   https://doi.org/10.1016/j.geomorph.2015.06.006 , 2015.

735 Yang, P., Wang, N. A., Zhao, L., Zhang, D., Zhao, H., Niu, Z., and Fan, G.: Variation
736   characteristics and influencing mechanism of CO2 flux from lakes in the Badain
737   Jaran Desert: A case study of Yindeer Lake. Ecol. Ind., 127, 107731,
738   https://doi.org/10.1016/j.ecolind.2021.107731 , 2021.

739 Yvon-Durocher, G., Caffrey, J. M., Cescatti, A., Dossena, M., Giorgio, P. D., Gasol, J.
740   M., ... and Allen, A. P.: Reconciling the temperature dependence of respiration
741   across timescales and ecosystem types. Nature, 487(7408), 472-476,
742   https://doi.org/10.1038/nature11205 , 2012.

743 Yvon-Durocher, G., Jones, J. I., Trimmer, M., Woodward, G. and Montoya, J. M:
744   Warming alters the metabolic balance of ecosystems. Phil. Trans. R. Soc. B 365,
745   2117–2126, https://doi.org/10.1098/rstb.2010.0038 , 2010.
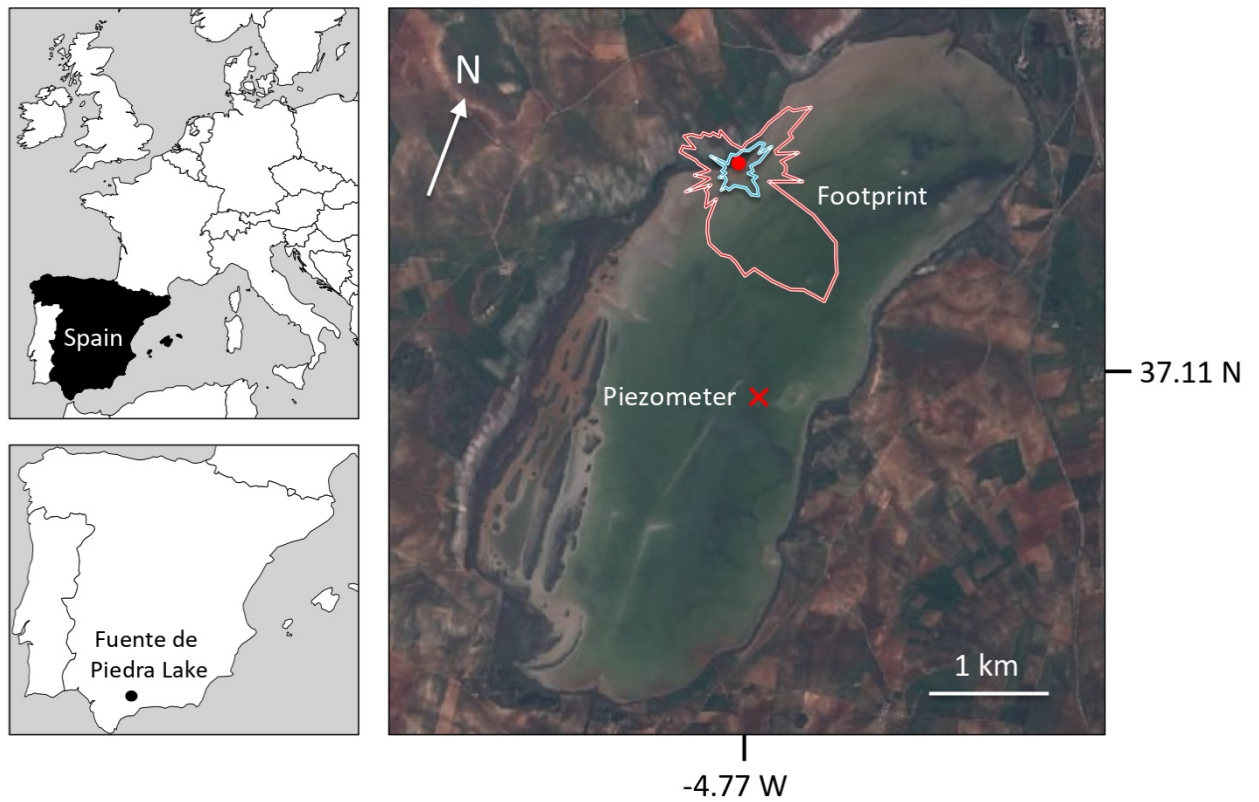
Fig 1. Location of the Fuente de Piedra Lake (province of Málaga, South of Spain). Dot inside polygon in right panel shows the location of the eddy covariance tower. The areas within the footprint contributing the 90% to measured fluxes are delimited inside polygons for daytime (blue) and nighttime (red). The cross indicates the location of the piezometer used for measuring groundwater level. Source image: Sentinel-2.
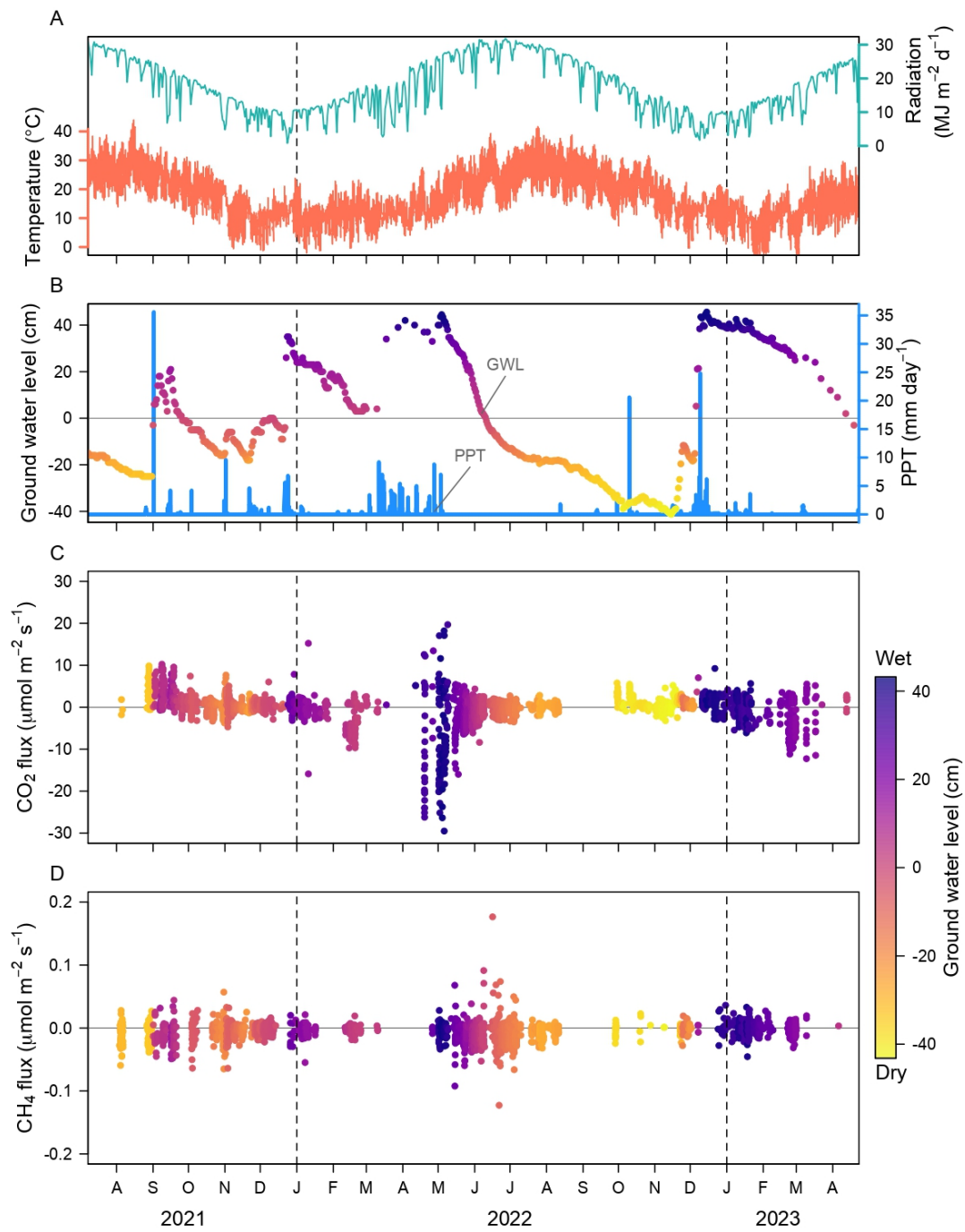
Fig 2. Time series of (A) air temperature and incident solar radiation, (B) groundwater level and precipitation (PPT), (C) CO_2 and (D) CH_4 flux, collected at Fuente de Piedra Lake during 2021, 2022, and 2023.
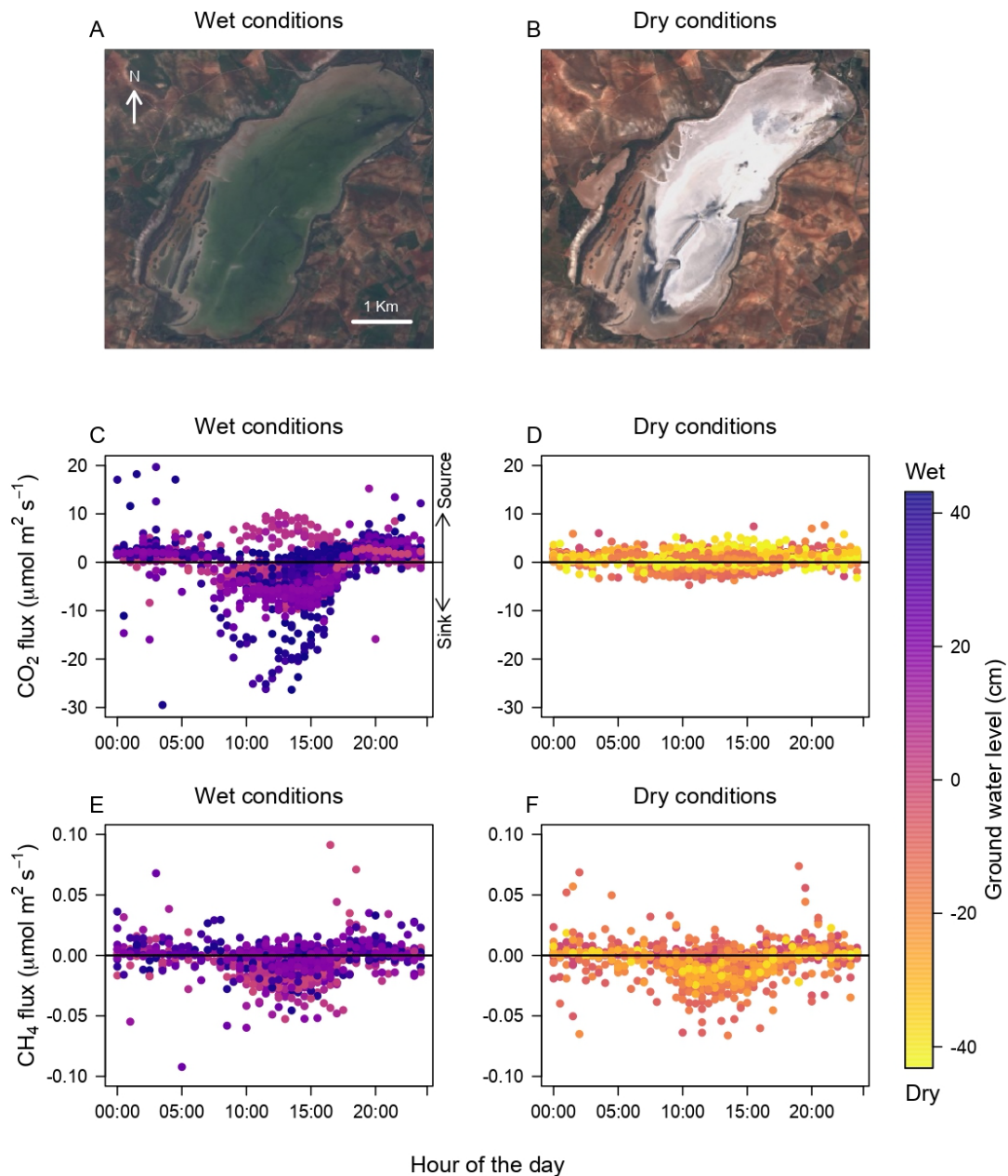
Fig 3. Aerial photos of Fuente de Piedra Lake during a period of maximum water availability (wet, **A**) and during a typical dry episode (**B**). Note that for some period during the dry episodes, a salt crust forms covering practically the entire extent of the lake. The figure shows the daily pattern of CO_2 and CH_4 fluxes during wet conditions (**C** and **E** respectively) and dry conditions (**D** and **F** respectively). Water availability is measured in terms of groundwater level. Source image: Sentinel-2. Wet image was taken on 17-02-2021 and dry image was taken on 13-5-2021.
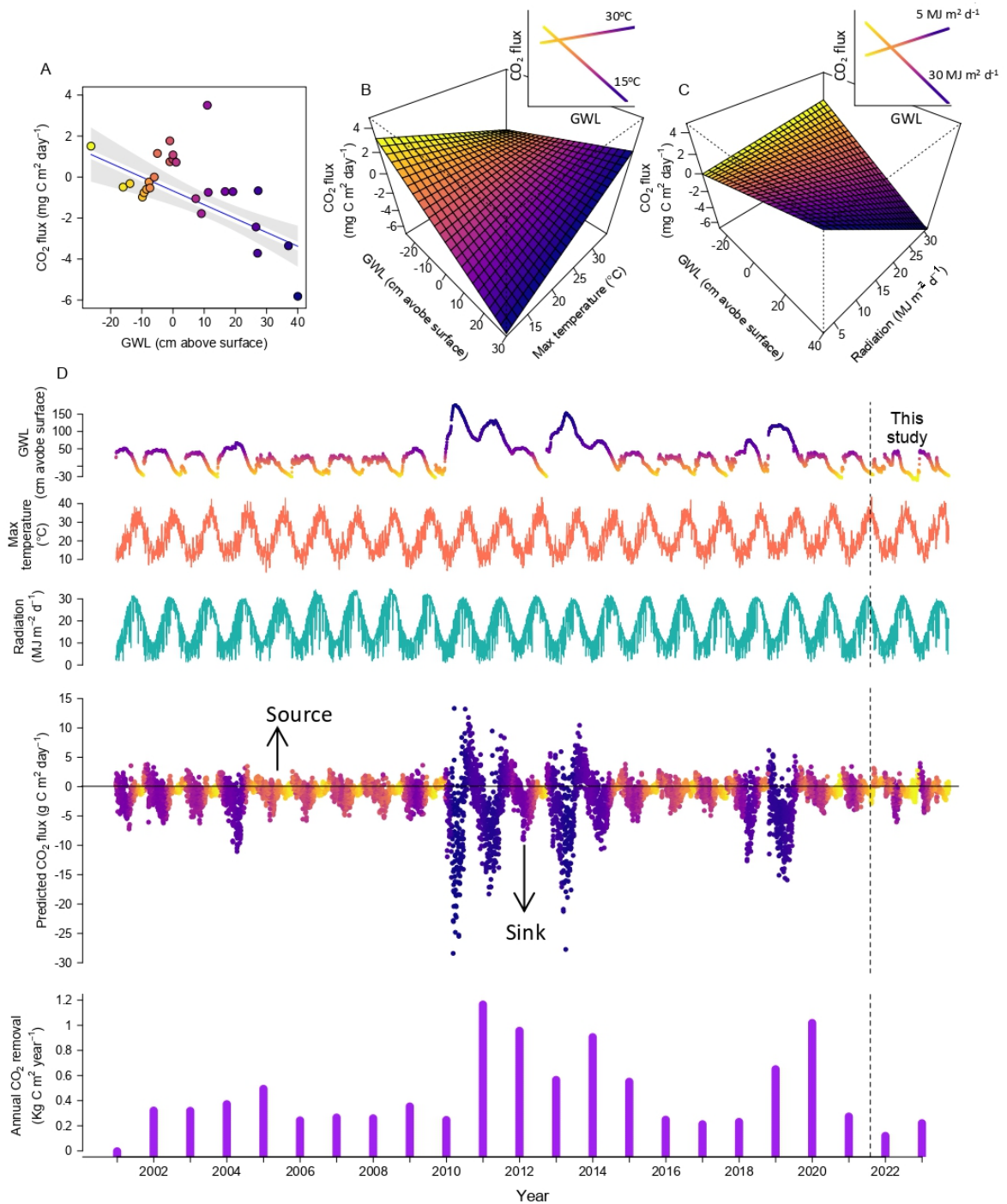
Fig 4. Prediction of CO_2 flux as a response to groundwater level with a slope of -0.115 (**A**), the interaction between groundwater level and daily maximum temperature (**B**), and the interaction between groundwater level and incident solar radiation (**C**). Model has an R^2 of 0.73. Using existing time series for the model predictors, it has been possible to reconstruct the estimated CO_2 fluxes, as well as the annual cumulative value of CO_2 removal since 2001 for Fuente de Piedra Lake (**D**).